ANNALS OF GEOPHYSICS, 61, 2, SE226, 2018; doi: 10.441/ag-7709

“SEISMIC AMPLIFICATION EFFECTS AND SOIL-TO-STRUCTURE INTERACTION STUDY NEARBY A FAULT ZONE: THE TREMESTIERI FAULT AND MADRE TERESA DI CALCUTTA SCHOOL (CATANIA)”

Mario Paratore[1,*], Luciano Zuccarello[1,2,3], Giuseppina Tusa[1], Danilo Contrafatto[1], Domenico Patanè[1]

[(1)] Istituto Nazionale di Geofisica e Vulcanologia, Osservatorio Etneo - Sezione di Catania, Catania, Italy
[(2)] Universidad de Granada, Dpto. de Teoría de la Señal, Telemática y Comunicaciones ETSI Informática y de Telecomunicación Universidad de Granada, Spain
[(3)] Instituto Andaluz de Geofisica, University of Granada, Granada, Spain

Article history
Receveid XMarch 21, 2017; accepted September 5, 2017.
Subject classification:
Seismic surveys; Seismic ambient noise; Fault zone; Resonant frequencies; Directional amplification.

ABSTRACT

Results of passive seismic surveys, in terms of both amplification and polarization effects in a section of the Tremestieri Etneo Fault (Sicily Eastern center - Catania) are discussed. For the purpose, velocimetric and accelerometric records of seismic ambient noise were analyzed. The polarization analysis of particle motion was performed and azimuthally dependent resonant frequencies were estimated. Ambient noise data were also used to assess the dynamic properties of a reinforced concrete building, located on the fault zone. The fundamental modes have been estimated through ambient noise recordings acquired by three-directional accelerometers, installed at the highest accessible floor and outside the building. The study revealed a clear oriented seismic amplification in the fault zone. This effect was observed in intensely jointed rock masses, located inside the fault area, as the result of specific geometries and significant directional impedance contrasts characterizing the area under study. The analyses show that the direction of the largest resonance motions has transversal relationship with the dominant fracture orientation. The directional amplification is inferred to be produced by stiffness anisotropy of the fault damage zone, with larger seismic motions high angle to the fractures. The results obtained are in complete agreement with those obtained by a previous study which analyzed the fault section located to the north-west.Finally, comparing the dynamic properties of the school building and the vibrational characteristics of the soil in the direction of maximum amplification, no clear resonant effect in the soil-structure interaction has been observed.

1. INTRODUCTION

The fault zones contain, in most cases, very extensive deformed rock portions with high degree of fracturing and presence of granular materials, which widths extend from tens to hundreds of meters transversely to the sliding line. Low elastic coefficient and low propagation velocity characterize these areas, whose immediate consequence is an amplification of the seismic motion. The fault zone can trap seismic waves amplified by constructive interference of the critically reflected phases [Ben-Zion and Aki 1990; Li and Leary 1990; Li et al., 1997]. This phenomenon has been observed on numerous active faults [Li et al., 1990; Ben Zion et al., 2003; Peng et al., 2003; Mizuno and Nishigami 2004; Lewis et al., 2005] and is often associated with a sharp polarization of motion. In general, one or more fracture systems can be developped within a fault zone, depending on the fault kinematics, stress field, rock rheology and other site-dependent factors. These fractures accommodate shear and dilatational brittle deformation fields that are organized into ‘fracture cleavage’ patterns [Caine et al., 1996]. In the medium, the presence of widespread microcraks parallel to the fault strike causes anisotropy of the elastic properties which are transversal to the sliding surfaces. This anisotropy should lead to ground motion amplification in the normal direction, or at high angle to the direction of sliding [Pischiutta et al., 2012].

Recent studies [e.g., Rigano et al., 2008] have shown

that the seismic signals are strongly polarized in the fault systems of Mount Etna with normal and strike-slip kinematics (e.g., Tremestieri fault, Pernicana fault, Moscarello and Acicatena fault). In these fault zones-the polarization of horizontal components of motion have an orthogonal relationship with the orientation of the main fractures, produced by the fault kinematics in the damage zone. Similarly, Di Giulio et al. [2009] found that the polarization angle of the horizontal component is not parallel to the discontinuity line between NE rift and the Pernicana fault. The authors interpreted it as "directional resonances" , attributing these anisotropic effects to microfractures occurring within the damage zones.

In this paper, we investigate polarization of amplified ground motion along the fault segment of Tremestieri Fault crossing the Tremestieri Etneo village, in the province of Catania),by analysing the seismic records acquired by the seismic stations installed both across and along the fault area,.. The seismic stations were installed by the "Istituto Nazionale di Geofisica e Vulcanologia" (INGV) as part of the research project POR-FESR *"Attività di sviluppo sperimentale finalizzata alla riduzione del rischio sismico nella Sicilia orientale"*, which took place between the years 2012 - 2015. The aim of this work was also to compare the dynamic elastic properties of a Reinforced Concrete (RC) building (test site of the above-mentioned research project and built on the fault zone damaged), with the vibrational characteristics of the underlying soil, in order to identify possible resonance phenomena. This resonance approach was introduced for microzonation studies of cities and it represents the first step to validate vulnerability models of buildings [Mucciarelli and Gallipoli, 2007].

2. GEOLOGICAL AND STRUCTURAL SETTING

Mount Etna volcano is one of the most active and well monitored volcanoes of the world, and is characterized by continuous ground deformation processes along significant portions of its flanks. There are several mechanisms which can be considered responsible for surface deformation. Between these, we can mention:

i) the load of the volcano, that produces continuous flank deformation;
ii) the magma accumulation, that induces uplift and tends to destabilize the E flank of the volcano;
iii) dike emplacements, that episodically affect the whole E flank of the volcano through transient acceleration periods [Solaro et al., 2010, and references therein].

The E flank of M. Etna represents the area affected by the major flank instability and where we found important fault systems such as the Pernicana Fault system, the Timpe Fault system and Tremestieri Fault system (Figure 1a). In particular, the Tremestieri Fault is a prominent structural element of the lower southeast flank of the M. Etna volcano. It is orientedtowards NNW-SSE and is characterized by clear morphological scarps. According to the most recent surveys [i.e. Azzaro, 2010], it mark the southern edge of the eastern flank of the volcano, highly unstable and subject to continuous slow sliding towards east and south-east [Ferrucci et al., 1993]. Moreover, the eastern flank of the volcano is affected by shallow and spatially restricted seismicity [e.g. Lo Giudice and Rasà, 1992; Lombardo and Cardaci, 1994]. In this frame, the Pernicana and the Tremestieri fault systems represent the discrete structural elements embracing the seaward sliding sector [Rasà et al., 1996]. In particular, the Tremestieri fault system is depicted both by right-handed strike-slip movements, and by normal movements of dip-slip. Along this fault, shallow earthquakes with typical focal depth of 1-2 km, low magnitude and apparent surface faulting have been recorded. The seismic energy is released through earthquake swarms as well as seismic creep phenomena [Lo Giudice and Rasà, 1992]. The most recent and important seismic activity occurred during the 1980 seismic sequence, indicating a right-lateral and oblique displacement that implied a left stepping secondary system of en-echelon cracks trending N45°E and accompanying the NW-SE trending ruptures [Azzaro, 1999].

The area of the Tremestieri village is extensively crossed by a segment of the Tremestieri fault. This area is characterized by lava flows and pyroclastic products, belonging to the "Pietracannone" and "Torre del Filosofo" formations. These formations include the lava events from 15 ka until 1669 [Branca et al., 2011] (Figure 1b). In particular, in the studied area the lava flows range between 3.9 ka - 122 BC and from 122 BC until 1669, relating to the San Giovanni La Punta and Monti Arsi di S. Maria lava flows [Imposa et al., 2013].

3. DATA ACQUISITION AND PROCESSING

In order to study the ground motion amplification and polarization across the Tremestieri Fault, we used eight ambient noise recordings, located both along the fault zone and at sites outside it, (Figure 2). spaced about 150 meters away from the displacement area. We want to point out that, strong evidences of the tectonic

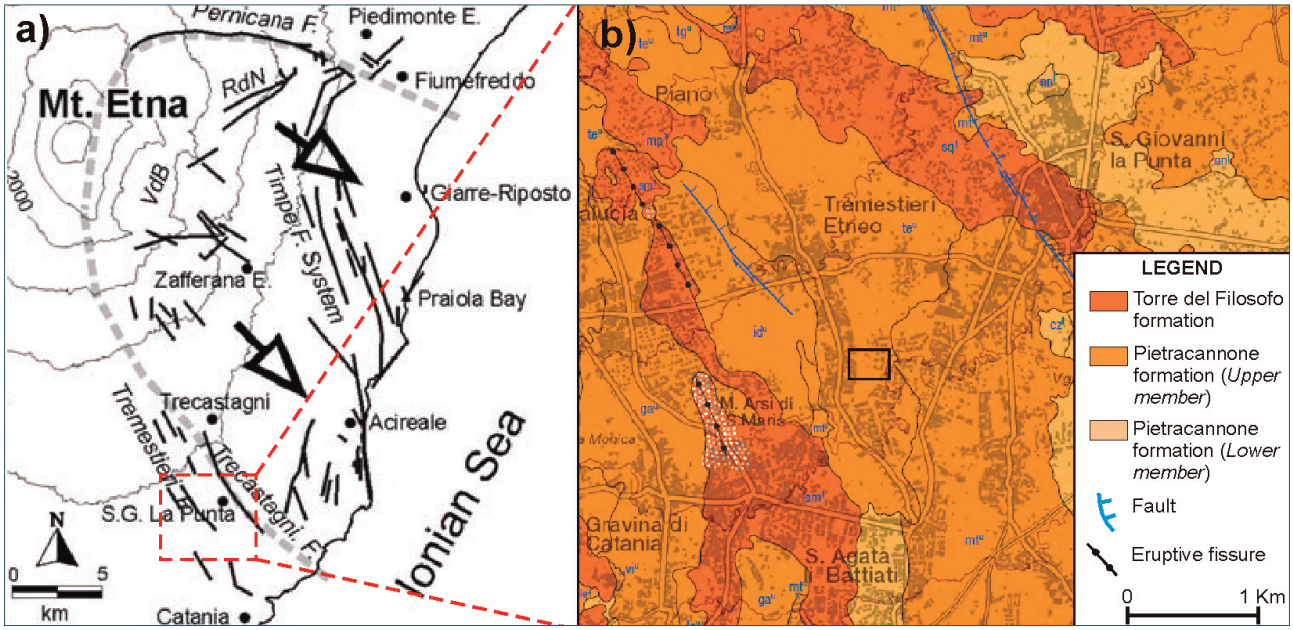

FIGURE 1. (a) Simplified structural map of the eastern flank of Mt. Etna volcano: RdN, Ripe della Naca; VdB, Valle dal Bove. The gray line identifies the sliding sector [Gambino et al., 2011]. (b) Geological and structural map of the studied area extracted from Branca et al., 2011. The black rectangle indicates the stations deployment area. The legend describes geological formations and discontinuities. For more details see the aforementioned paper.

activity of the structure on several buildings, walls, roads and land were observed during our study, allowing us to plot the fault trace. Close to the Madre Teresa di Calcutta's school, surface deformations were found both on the road and on the ground outside the school.

Microtremor measurements were recorded using three portable seismic stations, equipped with three-component broadband seismometer sensors (Nanometrics Trillium Compact 120s; http://www.nanometrics.ca)

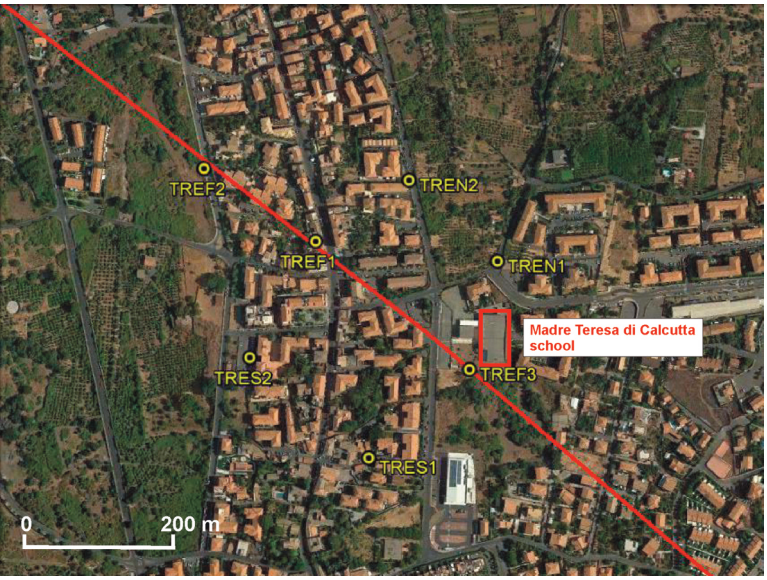

FIGURE 2. Localization of mobile seismic stations and the Madre Teresa di Calcutta school. Red line indicates the fault trace identified by surface evidence.

and three-component accelerometer sensors (Nanometrics Titan; http://www.nanometrics.ca). (Nanometrics Centaur; http://www.nanometrics.ca). The signals are digitized by a 24-bit A/D converter (Nanometrics Centaur; http://www.nanometrics.ca) with a sampling rate of 200 Hz. The time series (two hours long) were baseline corrected in order to remove spurious offsets and low-frequency trends. After the application of a Hanning window, a Fast Fourier Transform algorithm was applied to obtain spectra in the frequency band 0.5–20 Hz.

To evaluate site effects, the analysis of both horizontal-to-vertical (H/V) curves from noise and directionality of ground motion was performed. For each seismic station, we have calculated the spectral ratio between the average of the horizontal and vertical components of ground motion by applying the Nakamura [1989] technique (Horizontal-to-Vertical Spectral Ratio method, HVSR) . Thanks to its low cost and speed of use, Nakamura's technique is widely applied to quickly assess amplification effects in a given area and its fundamental frequency, even under site conditions different from those originally proposed. In particular, the use of spectral ratio after rotation of the horizontal components was first introduced by Spudich et al. [1996], and diffusely applied for detecting the horizontal polarization of ground motion in fault zones [e.g., Rigano et al., 2008; Di Giulio et al., 2009].

In this study, the signals were processed using the Geopsy software (www.geopsy.org) in order to evaluate

the spectral ratios between the ground motion components and investigate the main directions of the resonance frequencies. The seismograms were divided in 60 s time windows (Hanning taper and Konno-Ohmachi smoothing type were applied) and were selected their stationary portions, removing the presence of transient signals (i.e. the anthropic noise) that can distort our results. Finally, the spectral ratios were calculated after rotating the NS and EW components by steps of 10°, from 0° (North) to 180° (South). This approach is powerful in enhancing, if any, the occurrence of site-specific directional effects.

To better quantify the horizontal polarization, the covariance matrix method was applied. The polarization analysis makes full use of the three-component vector field to characterize the particle motion [Kanasewich, 1981; Bataille and Chiu, 1991]. The algorithm is applied in the time domain and is based on the eigenanalysis of the data covariance matrix. The covariance matrices are calculated for sliding time windows, which should be long enough to permit noise attenuation but should not include multiple signals. The seismic signals were previously filtered in the frequency band ranges from 2.5 to 3.5 Hz . The eigenanalysis provides a decomposition of the windowed data into their principal energy components [Samson, 1983; Jackson et al., 1991] given by eigenvalue–eigenvector pairs. The eigenvalues are the energy components, meanwhile the eigenvectors are the corresponding principal directions, which define both the axis length and orientation of the polarization ellipsoid. The linear or elliptical motions are projected on to one or two principal directions, respectively. For highly linear particle motion, the covariance matrix is dominated by one large eigenvalue, and the corresponding eigenvector represent the prevailing particle-motion orientation. The polarization analysis of the vector wave field provides three parameters that define particle motion:

(i) linearity, that quantifies the degree of linear alignment of the particle motion;
(ii) azimuth;
(iii) dip, which together describe the direction of the particle motion.

4. RESULTS

To evaluate the results, we have divided the diagrams of the spectral ratios into ”on-fault”, if the recording stations were located within a range of few meters around the fault trace, and ”off-fault” if placed at a distance of 150 m from the inferred fault plane (Figure 3). This representation, already used by Pischiutta et al. [2012], is particularly suitable for the overall observation of the results, especially relative to the longitudinal fault section. In the Figure 3, we show the average horizontal to vertical spectral ratios together with the contour plots of the spectral ratios for different rotation angles (from 0° to 180°) for the most representative stations. These contour maps highlight the presence of an important directional site effect since the H/V spectral ratio amplitude depends on the azimuth. Going through them in detail, we observe that the spectral analysis of the recorded signals from the on-fault stations highlights agreement on the results. In fact, in all H/V spectral ratios a dominant peak at the frequency of 3 Hz was found, with amplitude more than 2. Furthermore, at the same frequency, the analysis of directionality also indicates that the HV ratio is amplified at about 45-60° with respect to the north (i.e. orthogonally to the fault line). These results confirm that the H/V ratios on the fault zone have a clear coherent peak, which well correlates with the first directional resonance frequency. Conversely, the off-fault stations show seismic noise amplification in a frequency band around 3-7 Hz and no directionality. Moreover, at these stations, the dominant frequency is not coherent from a station to another, and the values of the spectral ratios in the NS component does not differ widely respect to EW (the H/V ratios vary from a minimum of 2 to a maximum of 3). On the contrary, in the on-fault stations, only the direction of maximum amplification shows resonance peaks. Indeed, the H/V ratio values are higher than 2 just around azimuthal direction of 60°.

In Figure 4 the azimuthal directions by rose diagrams are represented for both off-fault and on-fault stations. In general, the polarization analysis confirms the results obtained by the spectral ratios analysis. The seismic signals recorded by the on-fault stations show marked steady polarization parameters over time and space, in which the main direction of ground motion amplitude is orthogonal to the fault strike. Outside the fault zone, the seismic noise is more scattered (see Figure 4, left panel), except for the TRES2 station in which the seismic signal shows about EW orientation, maybe due to the an anthropic sources (heavy traffic roads in the east and west areas of the site) or to the presence of other fault segments in its proximity [Panzera et al., 2016, 2017].

5. DYNAMIC PROPERTIES OF A BUILDING LOCATED IN THE FAULT AREA

In the present study, we have evaluated the dynamic response of a building placed in the fault zone, with the aim of both evaluating the interaction with the underlying soils and identifying possible resonance phenom-

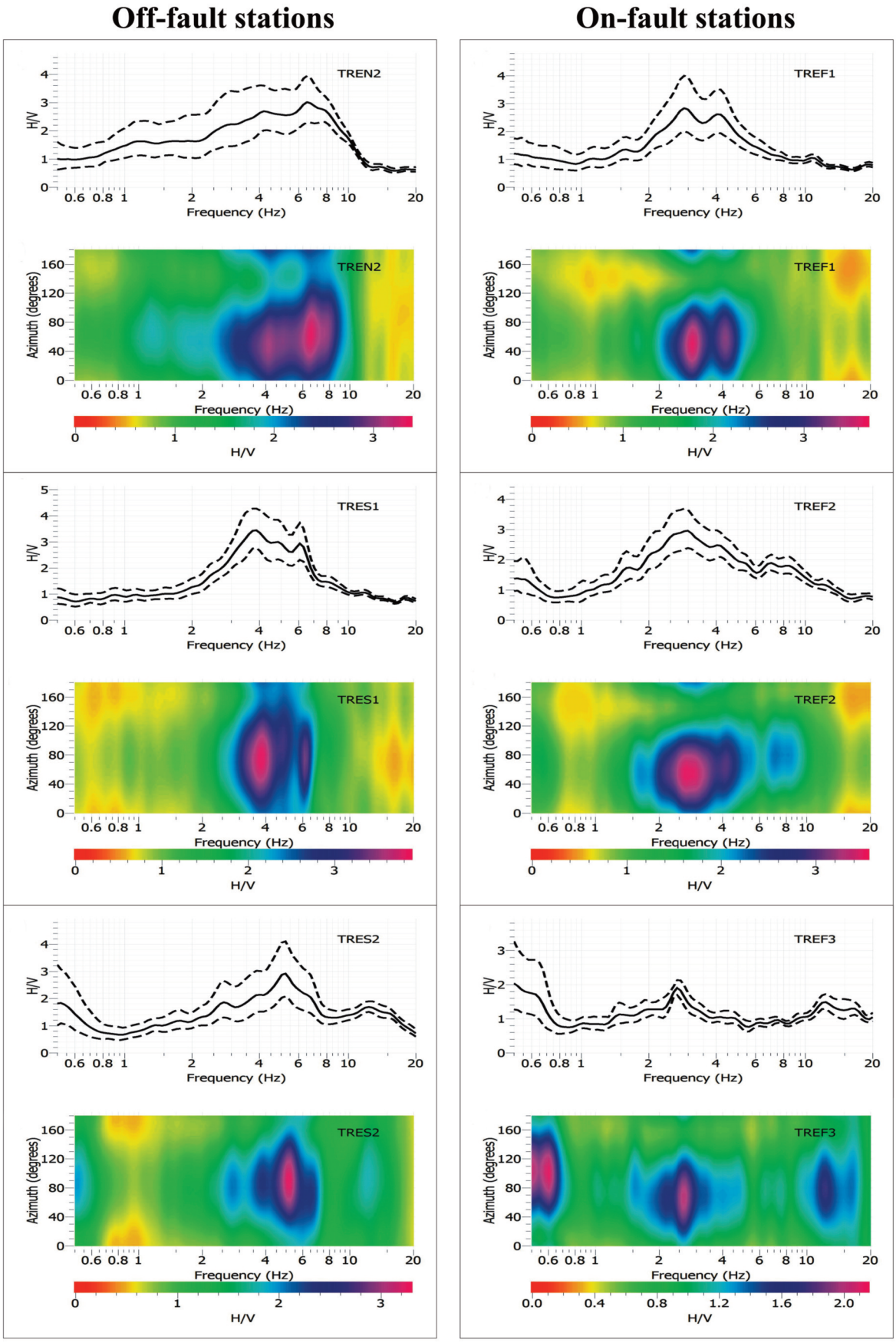

FIGURE 3. Horizontal-to-vertical spectral ratios of seismic signals recorded at each seismic station. In the upper panels, average spectral ratios (black line) and confidence intervals (black dotted lines) are drawn. In the bottom panels, the contour plots of the spectral ratios for different rotation angles are shown.

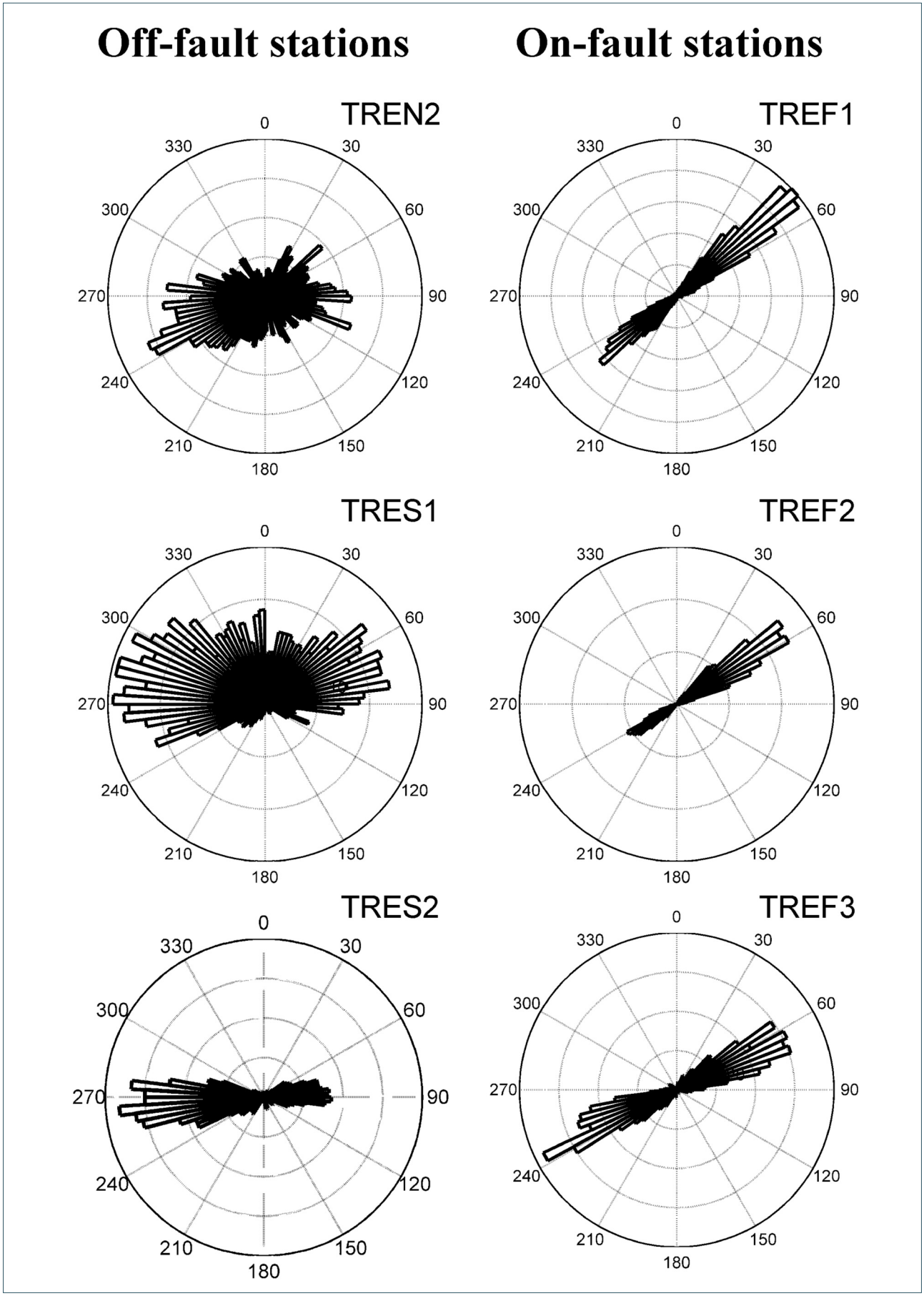

FIGURE 4. Off-fault (left column) and on-fault (right column) rose diagrams showing the horizontal polarization angles computed through the covariance matrix analysis.

ena. It is a reinforced concrete building, consisting of two floors, where the primary school "Madre Teresa di Calcutta" is housed (Figure 2). The best method to determine the dynamic parameters is using recording of earthquakes collected by a permanent monitoring system located inside the building. However, this approach requires observations of very long period. Alternatively, by using temporary stations, noise analysis can be applied.. The use of a portable instrument allows us to study the identification of structural dynamic characteristics: ambient vibrations are very useful for the characterization of the fundamental frequency and the related damping ratio, which represent the first fundamental parameters to validate vulnerability models. During the first step of the study, the fundamental frequencies of the building have been estimated using ambient noise recordings by means of a 3D accelerometer suitable to record ambient noise vibration (Kinemetrics Episensor FBA ES-T; https://kinemetrics.com/). The measurement has been carried out at the highest accessible floor; simultaneously, ambient noise measurements were performed outside the building by using a portable seismic station, equipped with three-component broadband seismometer sensor (station s/n E6027; Ibanez et al., 2016; Zuccarello et al., 2018). During data acquisition (lasting about two weeks), the accelerometer was placed as close as possible to the RC frame to minimize vertical modes of beams or floors. The sensor was oriented with respect to the Nord. Coincidently, the horizontal axes of the sensor correspond to the main directions of the building (that is the major axis ≡ NS direction and the minor axis ≡ EW direction) (see Figure 2). In Zuccarello et al. [2017] the fundamental periods of the building were estimated through the application of HVSR technique, by using the signals recorded both at the highest floor and the reference site outside the building. This methodology represents a very useful tool for estimating the dynamic properties of buildings, as shown in many studies where the results obtained from several experimental techniques were compared [e.g., Oliveira and Navarro, 2009; Gallipoli et al., 2009, 2010].

In addition, in order to better identify the building frequencies and the related directions in the horizontal plane, the rotational HVSR technique has been applied. In our case, this analysis is very important because the structure is placed in a fault damage zone where an oriented seismic amplification was observed. Figure 5 shows the obtained HVSR function (Figure 5a) and the rotational one (Figure 5b). The HVSR function has a very pronounced peak at the frequency of 6.8 Hz, representing the first flexional mode. Observing the directional diagram, it is possible to estimate the building fundamental frequency with a very good reliability: the fundamental frequency (6.8 Hz) appears rotated by 165° with respect to the north direction. A second peak (less intense) can be observed at 2.7 Hz, rotated by almost 50° with respect to the north. This value is due to the soil contribution, as demonstrated by the comparison between the directional contour diagrams obtained from seismic data recorded on the building and those in free-field conditions (see Figure 3, TREF3 Station).

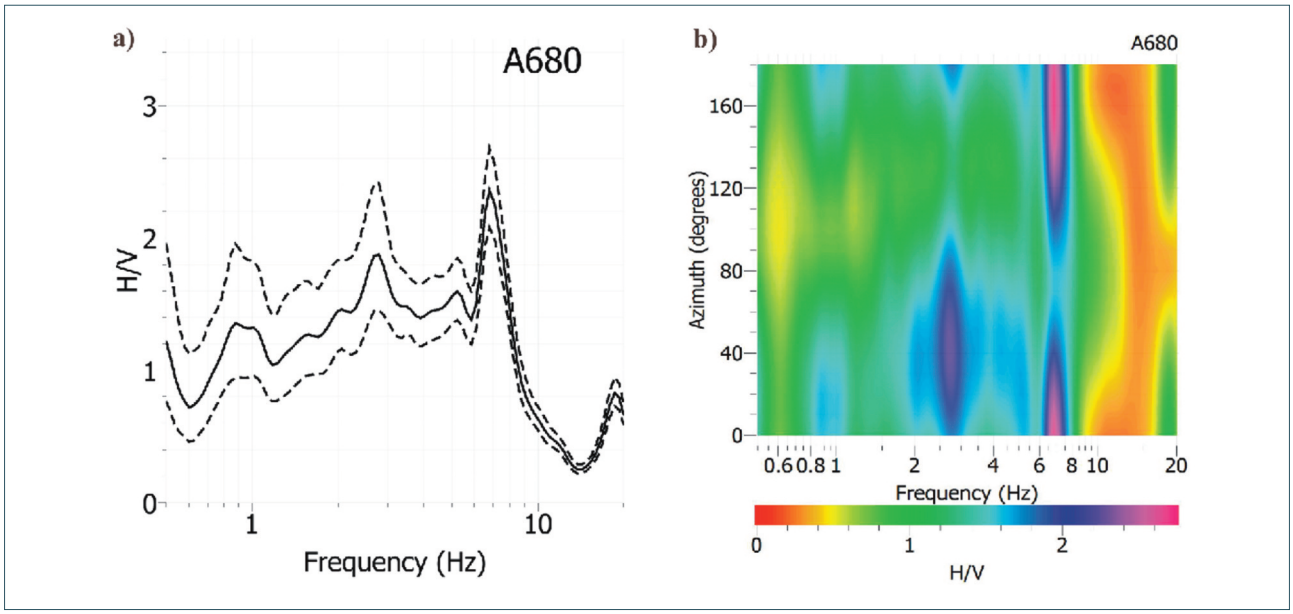

FIGURE 5. Horizontal-to-vertical spectral ratio (a) and contour plot of H/V amplitudes with rotation angle versus frequencies (b) from seismic noise data recorded at top floor of Madre Teresa di Calcutta school.

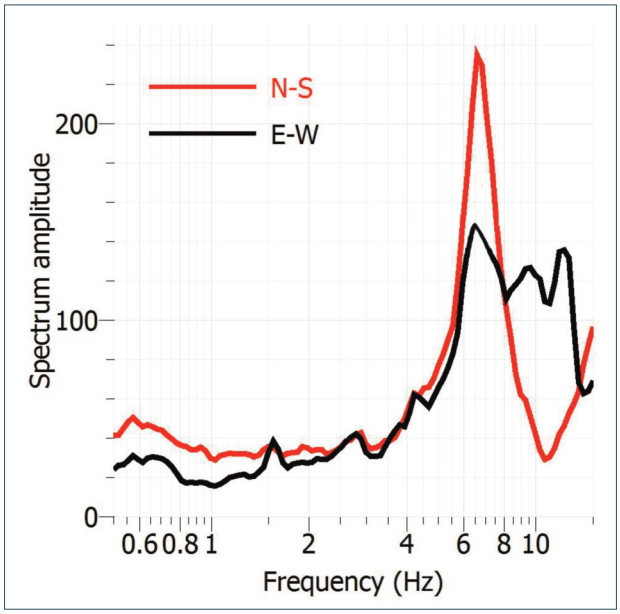

FIGURE 6. Fourier spectra evaluated along the north-south (red line) and east-west (black line) directions.

The results obtained by HVSR technique were compared with the Fourier spectra evaluated along the horizontal components (Figure 6). The spectral analysis confirms an amplitude peak at the frequency of 6.6 Hz in both horizontal components, consistent with the results from the HVSR analysis. Subsequently, the damping ratio of the building was determined using ambient noise measurements by the Random Decrement Method (RDM). This analysis is conducted in the time domain by measuring the logarithmic decrement of an oscillating system following the initial displacement from an unknown random source, as for instance the microtremor [Cole, 1973]. The average of a large number of temporal signal segments, defined from a trigger value, has been assessed. The total response of a system to random sources is given by the sum of three components: (1) response due to the initial displacement; (2) response due to the initial velocity; (3) forcing function. By averaging a high number of segments, the last two components are canceled and just the component (1) remains which represents the real response of a linear system to an initial displacement [Yang et al., 1983]. This technique is valid for a system with a single degree of freedom. To maintain this condition, we used a bandpass filter calibrated on the system frequency (6-8 Hz). We also selected the size of stacked window (2 s) containing more than ten periods. Figure 7 shows the decay curves of the motion components (vertical, north-south, east-west) and corresponding damping values percentage. On the north-south component, the fundamental frequency obtained through

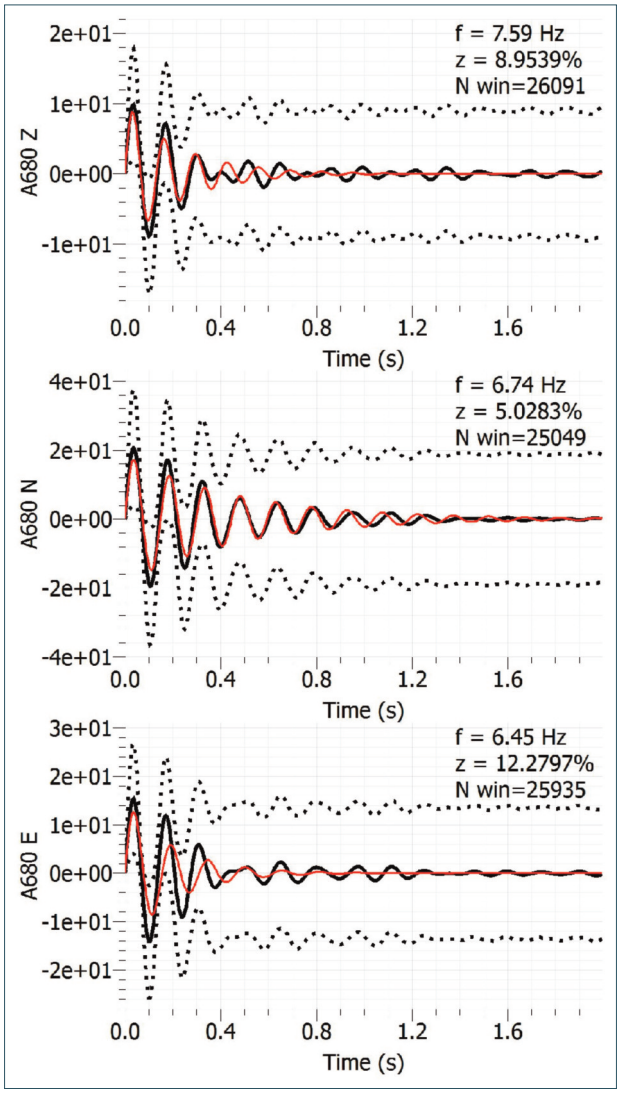

FIGURE 7. Decay curves of the motion components using Random Decrement Method (RDM). Each panel shows the corresponding frequency, damping values percentage and number of the stacked windows.

the RDM technique was 6.74 Hz with damping of about 5%, while on the east-west component was 6.45 Hz with damping of about 12%. The frequency values are quite similar to the ones obtained through the HVSR method and Fourier spectra. The values of the viscous damping are different and associated with the stiffness of the structure in the considered direction. It follows that in the N-S direction the building is characterized by higher stiffness respect to the E-W one.

6. CONCLUSIONS

The results obtained by ambient noise analysis indicates that in the Tremestieri fault damage zone the lavas amplify the ground motion. In particular, the

polarization analysis shows a dominant azimuthal angle persisting along the fault segment. Considering the structural characteristics of the Tremestieri fault (N125E strike and right-lateral movement), the observed particle motion oriented N45°E-N60°E, suggests a substantially perpendicular relation between the wave polarization azimuth and the strike of the fracture cleavage in the fault damage zone. These results are in good agreement with what Lombardo and Rigano [2006] found. In particular, the authors analyzed the ambient noise recorded in three profiles crossed by Tremestieri fault (westernmost part of our studying area), and observed an amplification of the seismic signals at 4.0 Hz. Furthermore, they showed that the resonance effect at 4.0 Hz is directional, with the maximum in the azimuth range N30E–N80E.

Evidences of ambient noise to be strongly polarized were found at all seismic stations placed along the fault. This persistent structural feature allow us to trace the fault damage zone on the east area of the Tremestieri village (in this area, no observation by seismic stations was made before), where a new building, housing a primary school, has been recently built. By comparing the dynamic properties of this building and the vibrational characteristics of the soil in the direction of maximum amplification, no clear resonant effect in the soil-structure interaction was possible to observe. However, it is necessary to highlight that the analyses performed on the building are related only to the closest portion of the fault line which is disconnected from the other sector, and characterized by the presence of an elevator shaft, (a structural element not present in the northern portion of the building).

Therefore, in the future, it should be important to install a new seismic station in order to compare the seismic response between the two sectors. It is important to mention that in this work the analyses carried out assess vibrational modes and their damping only in the elastic domain. No assessment can be made of structural damage conditions, in which the dynamic features significantly differ.

Our study confirms that fault zone can become place of seismic amplification. In particular, it was observed that the horizontal ground motion increases up to a factor of about 3 (see spectral amplitudes), in the perpendicular direction to the fault line. The experimental technique allows to highlight the presence of site effects and their spatial distribution. This becomes an important and additional element to consider in seismic risk and the seismic microzoning studies for territorial planning.

Acknowledgements. This paper has been funded by the following research projects: "Attività di sviluppo sperimentale finalizzata alla riduzione del rischio sismico nella Sicilia Orientale" inside the PO-FESR 2007-2013 Sicilia; MED-SUV funded from the European Union Seventh Framework Programme (FP7) under Grant agreement n°308665. This work is sponsored by European Union's Horizon 2020 research and innovation programme under the Marie Sklodowska-Curie grant agreement n° 798480.

REFERENCES

Azzaro, R. (1999). Earthquake surface faulting at Mount Etna volcano (Sicily) and implications for active tectonics, J. Geodyn. 28, 193-213.

Azzaro, R. (2010). "Sismicità ed effetti dei terremoti nel versante orientale dell'Etna"-Microzonazione sismica del versante orientale dell'Etna. Studi di primo livello, Regione Siciliana, Dipartimento della Protezione Civile - Le Nove Muse Editrice.

Bataille, K. and J. M. Chiu (1991). Polarization analysis of high-frequency, three-component seismic data, Bull. Seism. Soc. Am., 81, 622-642.

Ben-Zion, Y. and K. Aki (1990). Seismic radiation from an SH line source in a laterally heterogeneous planar fault zone, Bull. Seism. Soc. Am., 80, 971-994.

Ben-Zion, Y., Z. Peng, D. Okaya, L. Seeber, J. G. Armbruster, N. Ozer, A. J. Michael, S. Baris and M. Aktar (2003). A shallow fault-zone structure illuminated by trapped waves in the Karadere-Duzce branch of the North Anatolian Fault, western Turkey, Geophys. J. Int., 152, 699-717.

Branca, S., M. Coltelli, G. Groppelli and F. Lentini (2011). Geological map of Etna volcano, 1:50,000 scale, Ital. J. Geosci., 130, 3, 265-291.

Caine, J. S., J. P. Evans and C. B. Forster (1996). Fault zone architecture and permeability structure, Geology, 24, 1025-1028.

Cole, H. A. (1973). On-line failure detection and damping measurements of aerospace structures by Random Decrement Signature, Technical Report, NASA-CR-2205, NASA, Washington, United States.

Di Giulio, G., F. Cara, A. Rovelli, G. Lombardo and R. Rigano (2009). Evidences for strong directional resonances in intensely deformed zones of the Pernicana fault, Mount Etna, Italy, J. geophys. Res., 114, doi:10.1029/2009JB006393.

Ferrucci, F., R. Rasà, G. Gaudiosi, R. Azzaro, and S. Imposa (1993). Mt. Etna: a model for the 1989 eruption, J. Volcanol. Geotherm. Res., 56, 35-56.

Gambino, S., A. Bonforte, A. Carnazzo, G. Falzone, F. Fer-

rari, A. Ferro, F. Guglielmino, G. Laudani, V. Maiolino and G. Puglisi (2011). Displacement across the Trecastagni Fault (Mt. Etna) and induced seismicity: the October 2009 to January 2010 episode, Ann. Geophys., 54, 4, doi:10.4401/ag-4841.

Gallipoli, M. R., M. Mucciarelli and M. Vona (2009). Empirical estimate of fundamental frequencies and damping for Italian buildings, Earthquake Engineering Structural Dynamics, 38, 973-988.

Gallipoli, M. R., M. Mucciarelli, B. Šket-Motnikar, P. Zupanćić, A. Gosar, S. Prevolnik, M. Herak, J. Stipčević, D. Herak, Z. Milutinović and T. Olumćeva (2010). Empirical estimates of dynamic parameters on a large set of European buildings, Bulletin of Earthquake Engineering, 8, 593-607.

Jackson, G. M., I. M. Mason and S. A. Greenhalgh (1991). Principal component transforms of triaxial recording by singular value decomposition, Geophysics, 56, 528-533.

Ibáñez, J.M., et al. (2016). TOMO-ETNA experiment at Etna volcano: activities on land, Ann. Geophys., 59, 4, S0427, doi:10.4401/ag-7080.

Imposa S, F. Fazio, S. Grassi and G. Rannisi (2013). Studio della risposta di sito in un area del versante meridionale del Mt. Etna, in: Geofisica Applicata, 2, 409-416, Trieste, 19-21 Novembre.

Kanasewich, E. R. (1981). Time Sequence Analysis in Geophysics, University of Alberta Press, Edmonton, 477.

Lewis, M. A., Z. Peng, Y. Ben-Zion and F. L. Vernon (2005). Shallow seismic trapping structure in the San Jacinto fault zone near Anza, California, Geophys. J. Int., 162, 867-881, doi:10.1111/j.1365-246X.2005. 02684.x.

Li, Y. G. and P. C. Leary (1990). Fault zone trapped seismic waves, Bull. Seism. Soc. Am., 80, 1245-1271.

Li, Y. G., P. C. Leary, K. Aki and P. Malin (1990). Seismic trapped modes in the Oroville and San Andreas fault zones, Science, 249, 763-765, doi:10.1126/science.249.4970.763.

Li, Y. L., G. W. Ellsworth, C. H. Thurber, P. E. Malin and K. Aki (1997). Observations of fault zone trapped waves excited by explosions at the San Andreas fault, central California, Bull. Seism. Soc. Am., 87, 210-221.

Lo Giudice, E., and R.Rasà (1992). Very shallow earthquakes and brittle deformation in active volcanic areas: the Etnean region as example, Tectonophysics, 202, 257-268.

Lombardo, G., and C. Cardaci (1994). The seismicity of the Etnean area and different features of observed seismic sequences, Acta Vulcanologica, 5, 155–163.Lombardo, G. and R. Rigano (2006). Amplification of ground motion in fault and fracture zones: Observations from the Tremestieri fault, Mt. Etna (Italy), J. Volcanol. Geotherm. Res., 153, 167-176.

Mizuno, T. and K. Nishigami (2004). Deep structure of the Mozumi-Sukenobu fault, central Japan, estimated from the subsurface array observation of fault zone trapped waves, Geophys. J. Int., 159, 622-642.

Mucciarelli M. and M. R. Gallipoli (2007). Non-parametric analysis of a single seismometric recordings to obtain building dynamic parameters, Ann. Geophys., 50, 259-266.

Nakamura, Y. (1989). A method for dynamic characteristics estimation of subsurface using microtremors on the ground surface, Quarterly Rept. RTRI, Jpn., 30, 25-33.

Oliveira C.S. and M. Navarro (2009). Fundamental periods of vibration of RC buildings in Portugal from in-situ experimental and numerical techniques, Bull. Earth. Eng., 8, 3, 609-642.

Panzera, F., G. Lombardo, E. Longo, H. Langer, S. Branca, R. Azzaro, V. Cicala and F. Trimarchi (2017). Exploratory seismic site response surveys in a complex geologic area: a case study from Mt. Etna volcano (southern Italy), Nat Hazards, 86, S385–S399, doi: 10.1007/s11069-016-2517-4.

Panzera F., G. Lombardo and C. Monaco, (2016). New evidence of wavefield polarization on fault zone in the lower NE slope of Mt. Etna. Ital. J. Geosci., 135, 2, 250-260 doi: 10.3301/IJG.2015.22.

Peng, Z., Y. Ben-Zion, A. J. Michael and L. Zhu (2003). Quantitative analysis of fault zone waves in the rupture zone of the Landers, 1992, California earthquake: evidence for a shallow trapping structure, Geophys. J. Int., 155, 1021-1041.

Pischiutta M., F. Salvini, J. Fletcher, A. Rovelli and Y. Ben-Zion (2012). Horizontal polarization of ground motion in the Hayward fault zone at Fremont, California: dominant fault-high-angle polarization and fault-induced cracks. Geophys. J. Int., 188, 1255-1272, doi: 10.1111/j.1365-246X.2011.05319.x

Rasà, R., R. Azzaro, O. Leonardi (1996). Aseismic creep on faults and flank instability at Mt. Etna volcano, Sicily. In: Volcano Instability on the Earth and Other Planets, Geological Society Special Publication, 110, edited by W. C. McGuire, A. P. Jones and J. Neuberg, 179-192.

Rigano, R., F. Cara, G. Lombardo and A. Rovelli (2008). Evidence of ground motion polarization on fault zones of Mount Etna volcano, J. Geophys. Res., 113, doi:10.1029/2007JB005574.

Samson, J. C. (1983). The spectral matrix, eigenvalues, and

principal components in the analysis of multichannel geophysical data, Ann. Geophys., 1, 115-119.

Solaro, G., V. Acocella, S. Pepe, J. Ruch, M. Neri and E. Sansosti (2010). Anatomy of an unstable volcano from InSAR: Multiple processes affecting flank instability at Mt. Etna, 1994–2008, J. Geophys. Res., 115, B10405, doi:10.1029/2009JB000820.

Spudich, P., M. Hellweg and H. K. Lee (1996). Directional topographic site response at Tarzana observed in aftershocks of the 1994 Northridge, California, earthquake: implications for mainshock motions, Bull. Seismol. Soc. Am., 86, S193-S208.

Yang, J. C. S., N. G. Dagalakis, G. C. Everstine and Y. F. Wang (1983). Measurement of structural damping using the random decrement technique, Shock Vibration Bull., 53, 4, 63-71.

Zuccarello, L., G. Tusa, M. Paratore, C. Musumeci and D. Patanè (2018). Structural control of buildings by geophysical monitoring and first approach to Earthquake Early Warning, Ann. Geophys. (submitted for publication in this volume).

*CORRESPONDING AUTHOR: Mario PARATORE,
Istituto Nazionale di Geofisica e Vulcanologia,
Osservatorio Etneo - Sezione di Catania
email: mario.paratore@ingv.it